Algorithm of diffraction for standing tree based on the uniform geometrical theory of diffraction

Yun-Jie Xu*
School of technology, Zhejiang Agricultural & Forestry University, Lin'an, China
Email: xyj9000@163.com

Wen-Bin Li
School of technology, Beijing Forestry University, Bei jing, China
Email: leewb@bjfu.edu.cn

Shu-Dong Xiu
School of technology, Zhejiang Agricultural & Forestry University, Lin'an, China
Email: sdxiu@zjfc.edu.cn

***Abstract*— The diffraction fields and the shadow of standing tree diffraction are solved by using polygons to approximately take the place and approximation as approximate substitutes of for the circle. The algorithm model of ray path tracing is computed by tracing the ray path on standing tree. Considering electromagnetic wave propagation, which a physical model of diffraction for a forest is constructed. The mathematical model of diffraction is presented using the uniform geometrical theory of diffraction(UTD). Moreover, the expression for diffraction loss is derived. The results were then applied to the fir. Simulation and analysis show the validity of the proposed model.**

***Index Terms*— UTD, standing tree, algorithm of diffraction**

I. INTRODUCTION

Continuous data acquisition on multi-standing trees, which are sampled from a forest and are less than 50 m away from one another, is achieved. Thus, the information transfer between sensors is fully implemented. The sensor has a data acquisition multi-interface connecting sensors for temperature, illumination, and soil moisture, among others, which are all placed at breast height, thereby achieving wireless communication through an organized meshwork between sensors. The system can be practically used in the dynamic monitoring of growing forest stock and in obtaining the biomass ranges of the trees growing in different directions. The information gathered using the proposed system are useful for policymaking on the prevention or control of forest fires [1].

Results show signal frequency, stem form and propagation direction etc influence the diffraction fields and the blind region of diffraction. In this paper, algorithm of the diffraction fields and the blind region of diffraction in plantation are presented by accounting for application of the electromagnetic waves propagation and experimentation.

II. PHYSICAL MODEL OF DIFFRACTION FOR STANDING TREE

Ray theories, like the Geometrical Theory of Diffraction (GTD) and its uniform version (UTD) [2], are a very useful approach to characterize the scattering from objects and to estimate the electromagnetic field in arbitrary complex environments. In such theories, the electromagnetic field is described in terms of rays arising from a source, propagating through the scenario and interacting with it. These rays can be reflected or diffracted by the objects around the source. When the environment is complex, considering only the (singly) wedge diffracted rays is usually inadequate to reach the desired accuracy, especially when observing in low-field shadow regions. Therefore it is necessary to introduce higher order diffraction mechanisms that consist in vertex and multiple edge diffracted rays.

Stem form is diverse, but as a whole it consists of the basal area of breast-height and the basal area of end long. The wireless sensor placed at a breast height of 1.3 m can be further lowered to the basal

Manuscript received September 11, 2011
* Corresponding author; E-mail: xyj9000@163.com

doi:10.4304/jsw.7.6.1351-1357

area in the current paper, so only the effects of the basal area of breast height are considered. Circular area expressions are used for the measurements of the basal area of breast height and standing wood volume, with an average error of ±3%.

Fig.1 is the cylindrical surface r (u, v), source point is p_t (u_1, v_1) in the cylindrical surface, field point is p_r (u_2, v_2). The interval[v_1, v_2] is divided into N segments along u=u_1, N-1section point to determine the N-1 items u coordinate line; Similarly, the interval [u_1, u_2] is divided into N segments along v = v_1, M-1 section point to determine the M-1 items v coordinate line, then these u lines and v lines intersect, the intersection of p_{ij} for all surfaces can be characterized by discretely. crawling process of ray lines is divided to M segments using v coordinates of M-1 items. namely ray tracing of the solution process is divided into M phase, phase variable K = 1, 2, 3, …, M[4].

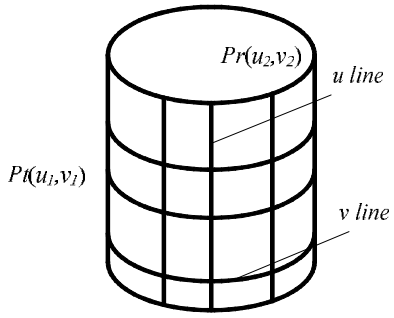

Figure 1. ray path tracing of standing tree

Phase 1 of the state S_1= {p_t}, Phase K of the state sets of value selection is intersection point set S_k = { p_{ij} [u_i , v_j] of coordinate net. Where i = K > 1 , j = 1 ,2 ,3 ,…, N} .

Phase K of the state sets of decision-making is intersection point set D_k = { p_{ij} [u_i , v_j] .

Based on the above section and variable definition, iteration relation of the ray tracing

$$f_{n+1}(s_{n+1}) = 0$$
$$f_k(s_k) = \min_{x_k \in D_k} \{d(s_k, x_k) + f_{k+1}(s_{k+1})\} \quad (1)$$

Where, k = n , n-1 , …,2 ,1; d (s_k , x_k) = n_k |$s_k x_k$| , n_k is refractive index, |$s_k x_k$| is the distance between two points.

Tracing calculation steps can be divided into four steps:

1)Discrete surface, Determine the coordinates p_{ij};

2)By using the substitution k = n+1 , f_k(s_k) = 0;

3)By using the substitution k=k–1, according to Eq. (1) yields f_k (s_k) and x_k , s_k∈{p_{kj}, j=1 , 2 ,…, m};

4)Repeat step until k=1, calculated f_1 (s_1) is the arc length of the track tracing ray, coordinates points of the ray after the reverse can also be found.

if cylindrical parameter equation:

$$r = (a\cos v, a\sin v, u) \quad (2)$$

according to the nature of cylindrical developable surface, ray path of the scene point source pr to field point pt is cylindrical spiral, arc length of ray is calculated as:

$$s = \sqrt{(u_2 - u_1)^2 + (v_2 - v_1)^2} \quad (3)$$

according to S yields N of Polygon edges. The model is shown in Fig.2, where(x_0, y_0, z_0) is source point , (x', y', z')is the secondary source point, (x_1,y_1,z_1)and (x_n, y_n, z_n)is the receiver point with the number border of polygon n, which is decided by tree's breed and diameter. The precision of the model increases with the increasing n. The radial can be divided into two components: one is that the incident energy propagates straightly according to the law of geometrical optics, and the other is that the incident energy propagates along the edge of stand tree, and the shadow and transition regions are formed when the radial of edge continual give off diffracted radial along the tangency. From the uniform geometrical theory of diffraction (UTD) introduce by P.H.Pathak and R.G.Kouyoymjian , that the region of transition is uniform. By accounting for application of the disposal of the sensor, we only consider the illuminated region and the shadow in this paper.

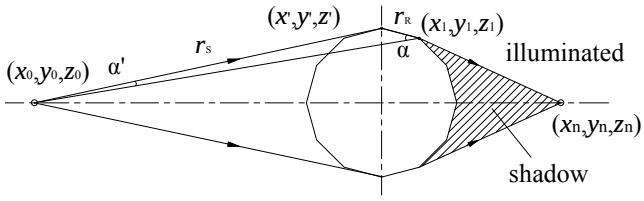

Figure 2. The simplified polygons model of standing tree

III. THE MATHEMATICAL MODEL OF DIFFRACTION FOR STANDING TREE

The problem of standing tree diffraction employing polygons to approximately take the place of the circle can be solved by the theory of diffraction through a wedge. To describe the diffraction effects caused by the edges of surfaces with the relatively simple mathematic method, we employ the Kirchhoff-Huygens approximation [8]. Huygens recognized that the fields reaching any precise surface between a source and receiver can be thought as the producing secondary point sources on the surface which in turn generate the received fields [9]. According to the Kirchhoff approximation, The receiver point(x_1,y_1,z_1) can be written as an integral for the complex amplitude over the plane x=0,which is given by

$$E\ (x_1, y_1, z_1) \approx \int_{-\infty}^{+\infty}\int_{-\infty}^{+\infty}[(\cos a + \cos a') \bullet$$

$$E^{inc}(0,y',z')\frac{jke^{-jkr_R}}{4pr_R}\Bigg]d_{y'}d_{z'} \quad (4)$$

Where r_R is the distance from the secondary source point in the plane x=0 to the receiver point (x', y', z') and E^{inc} is the amplitude of the secondary source.

The problem of diffraction of a plane wave by an edge through a wedge serves as a prototype for diffraction of electromagnetic waves through standing tree. As shown in Figure.2, due to r_s>>r_R, the distance from the source to y-axis is much larger than that of the receiving point to the y-axis, thus wave generated by source is approximately considered as the plane wave entering from the left to the fringe with x=0 of standing tree. Considering uneven surface of trees, the fringe of standing tree is simplified as an absorbing screen. To discuss the diffraction through effective angle, we consider the Z component of the field E and the polarization of the plane wave. If the plane wave propagates along the x-axis and r_s>>r_R, then the incident angle α'=0, thus the model can be further simplified shown in Fig.3. Where α' is diffraction angle and the wedge angle β = (2-n) π (1<n<2). The location of the angle α below the x-axis is the shadow boundary, and the shadow region below the boundary exists only the diffraction field.

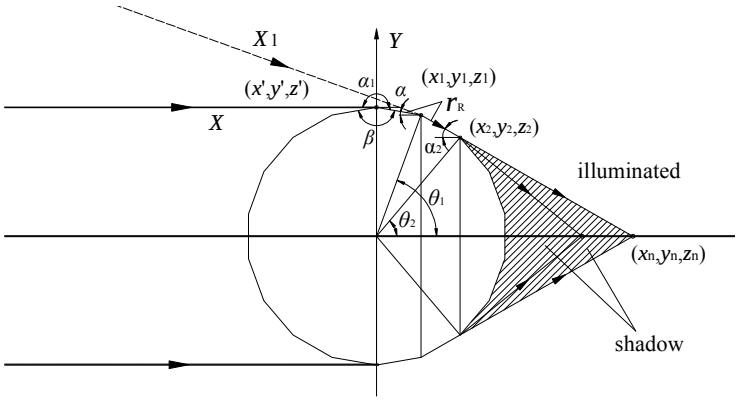

Figure 3. The simplified model of wedge diffraction

The Z component of the appropriate incident field will have spatial dependence given by

$$E^{inc}=A_0e^{-jkx} \quad (5)$$

Without loss of generality, the receiver points are assumed to lie in the plane Z=0 because of the translation symmetry along Z (trunk height direction). With the foregoing assumptions, the diffracted field through the edge for standing tree is given by

$$E(x_1,y_1,0)=A_0\frac{jk}{4p}\int_0^{+\infty}\int_{-\infty}^{+\infty}(1+\cos a)\frac{e^{-jkr_R}}{r_R}d_{z'}d_{y'} \quad (6)$$

Where the distance from the integration point to the receiver point is:

$$r_R=\sqrt{x_1^2+(y_1-y')^2+(z')^2} \quad (7)$$

To carry out the z' integration in (6), the primary contribution to the integral comes from a region of z' that is given by the Fresnel zone, which is small compared with x, i.e. x>>λ. The center of this region is the atationary-phase point where the derivative of the exponent k_{rR} with respect to z vanishes. r_R in the denominator of (7) and cosα will hardly vary and can be treated as constants.

Eq.(7) can be expanded to second order according to ρ_R with $r_R=\sqrt{x_1^2+(y_1-y')^2}$, and thus $r_R=r_R+\frac{(z')^2}{2r_R}$.

Substituting r_R into (3), the integration over z' in (6) reduces to

$$\begin{aligned}E(x_1,y_1,0)&=A_0\frac{jk}{4p}\int_0^{+\infty}\int_{-\infty}^{+\infty}(1+\cos a)\frac{e^{-jkr_R}}{r_R}d_{z'}d_{y'}\\ E(x_1,y_1,0)&\approx A_0\frac{jk}{4p}\int_0^{+\infty}(1+\cos a)\frac{e^{-jkr_R}}{r_R}\bullet\\ &\left[\int_{-\infty}^{+\infty}\exp\left[-jk\frac{(z')^2}{2r_R}\right]dz'\right]dy'\end{aligned} \quad (8)$$

By using the substitution $u=z'e^{jp/4}\sqrt{k/2r_R}$ to carry out integral transform, equation (8) changes into

$$\begin{aligned}E(x_1,y_1,0)&\approx A_0\frac{jk}{4p}\int_0^{+\infty}(1+\cos a)\frac{e^{-jkr_R}}{r_R}e^{jp/4}\sqrt{\frac{2pr_R}{k}}dy'\\ &=A_0\frac{e^{jp/4}}{2}\sqrt{\frac{k}{2p}}\left[\int_{-\infty}^{+\infty}(1+\cos a)\frac{e^{-jkr_R}}{\sqrt{r_R}}dy'\right]\\ &\quad-\int_0^{+\infty}(1+\cos a)\frac{e^{-jkr_R}}{\sqrt{r_R}}dy'\\ &=A_0\frac{e^{jp/4}}{2}\sqrt{\frac{k}{2p}}\int_0^{+\infty}(1+\cos a)\frac{e^{-jkr_R}}{\sqrt{r_R}}dy'\end{aligned} \quad (9)$$

Similarly, the expression $r_R=\sqrt{x_1^2+(y_1-y')^2}$ can be

expanded to second order as $r_R = r - y'\frac{y_1}{r}$ according to ρ with $r = \sqrt{x_1^2 + y_1^2}$. Here θ_1 is the angle between the X axis and the line from the edge to the receiver point, thus $\sin\theta_1 = y_1/\rho$.

By using the substitution $v = y'e^{-jp/4}\sqrt{k/r}$ to carry out integral transform, equation (9) turns into

$$\begin{aligned} E(x_1, y_1, 0) &= A_0 \frac{e^{jp/4}}{2}\sqrt{\frac{k}{2p}}\left[\int_0^{+\infty}(1+\cos a)\frac{e^{-jkr_R}}{\sqrt{r_R}}dy'\right] \\ &\approx A_0 \frac{e^{jp/4}}{2}\sqrt{\frac{k}{2p}}(1+\cos q)\frac{e^{-jkr}}{\sqrt{r}}\int_0^{+\infty}\exp\left(jky'\frac{y}{r}\right)dy' \\ &= A_0 e^{-jkr}\bullet\left(-\frac{e^{jp/4}}{\sqrt{2pkr}}\frac{1+\cos q}{2\sin q}\right) \end{aligned} \tag{10}$$

When carrying out the integration in (10), k is given a vanishingly small negative imaginary part, as appropriate for atmospheric absorption, to ensure convergence at the lower limit, but after the integration, k can be taken to be real. Let the diffraction coefficient $D(q_1) = -e^{jp/4}(1+\cos q_1)/(2\sin q_1\sqrt{2pkr})$, and substituting Eq. (5) into Eq.(10) yields

$$E(x_1, y_1, 0) = A_0 e^{-jkr} D(q_1) = E^{\text{inc}}(0, y', z')e^{-jkr} D(q_1) \tag{11}$$

In Fig.3., (x_1, y_1, z_1) is the secondary source point and (x_2, y_2, z_2) is the receiver point. The receiver field is given by

$$\begin{aligned} E(x_2, y_2, z_2) \approx \int_{-\infty}^{+\infty}\int_{-\infty}^{+\infty}(\cos a_2 + \cos a')\bullet \\ E^{inc}(x_1, y_1, 0)\frac{jke^{-jkr_R}}{4pr_R}d_{y_1}d_{z_1} \end{aligned} \tag{12}$$

The expression $r_R = \sqrt{x_2^{\,2} + (y_2 - y_1)^2 + (z_1)^2}$ can be expanded to second order as $r_R = r_R + \frac{(z_1)^2}{2r_R}$ according to r_R with $r_R = \sqrt{x_2^2 + (y_2 - y_1)^2}$, and the incident angle $a' = 0$.

Substituting r_R into (12) and integrating over z_1 in (12) reduces to

$$\begin{aligned} E(x_2, y_2, 0) \approx E^{inc}(x_1, y_1, 0)\frac{jk}{4p}\bullet \\ \int_0^{+\infty}(1+\cos a_2)\frac{e^{-jkr_R}}{r_R}\left[\int_{-\infty}^{+\infty}\exp\left[-jk\frac{(z_1)^2}{2r_R}\right]dz_1\right]dy_1 \end{aligned} \tag{13}$$

By using the expression $u = z_1 e^{jp/4}\sqrt{k/2r_R}$ to carry out integral transform, equation (13) changes into

$$\begin{aligned} E(x_2, y_2, 0) \approx E^{inc}(x_1, y_1, 0)\frac{e^{jp/4}}{2}\sqrt{\frac{k}{2p}}\bullet \\ \int_0^{+\infty}(1+\cos a_2)\frac{e^{-jkr_R}}{\sqrt{r_R}}dy_1 \end{aligned} \tag{14}$$

Similarly, the expression $r_R = \sqrt{x_2^2 + (y_2 - y_1)^2}$ can be expanded to second order according to ρ with $r = \sqrt{x_2^2 + y_2^2} = \sqrt{x_1^2 + y_1^2}$, then $r_R = r - y_1 y_2 / r$. Here θ_2 is the angle between the X' axis and the line from the edge to the receiver point, and thus $\sin\theta_2 = y_2/\rho$, where $\theta_2 = \theta_1 - 2\pi/n$, $n = 2m$ with the integer $m \geq 3$.

By using the expression $v = y_1 e^{-jp/4}\sqrt{k/r}$ to carry out integral transform, equation (14) turns into

$$\begin{aligned} E(x_2, y_2, 0) &= E^{inc}(x_1, y_1, 0)e^{-jkr}\bullet\left(-\frac{e^{jp/4}}{\sqrt{2pkr}}\frac{1+\cos q_2}{2\sin q_2}\right) \\ &= E^{inc}(x_1, y_1, 0)D(q_2)e^{-jkr} \end{aligned} \tag{15}$$

Where the diffraction coefficient $D(q_2) = -e^{jp/4}\bullet(1+\cos q_2)/(2\sin q_2\sqrt{2pkr})$.

Accounting for the influence of the diffusion factor A(s) and according to UDT, the approach described above can also be used to derive the field at the receiver point of (x_n, y_n, z_n), i.e.

$$E^n(s) = E^{n-1}(Q)D(q_n)A(s)\exp(-jks) \tag{16}$$

where $E^n(s)$ represents the diffraction field of the location s distance from the diffraction point Q, $E^n(Q)$ represents incident end-field of the radial at the diffraction point Q, $D(q_n)$ is the diffraction coefficient, the diffusion factor $A(s) = 1/\sqrt{s}$, $\exp(-jks)$ is the phase delay factor, and the wave number $k = 2p/l$.

When the diffraction field for an edge is calculated, one at first derives diffraction coefficient $D(q_n)$ at the diffraction point Q and the incident end-field $E(Q)$, then obtains the diffraction first-field at the diffraction point Q, and at last calculates the diffraction field of the location s distance from the diffraction point by employing the diffusion factor $A(s)$ and the phase delay factor $\exp(-jks)$. Form Eq. (16), we can see that the most important assignment is to derive the diffraction coefficient for calculating the diffraction field after we confirm the trajectory of diffraction radial.

Diffraction occurs when the radio path between the transmitter and the receiver is obstructed by a surface that has edges. In a forest, the primary diffracting obstacles, which perturb the propagating fields are trees. Diffraction formulas are well established for perfectly conducting infinite wedges [14, 15], for absorbing wedges, and for impedance-surface wedges [16]. The perfectly conducting diffraction coefficients are accurate when dealing with diffraction phenomena arising from metallic objects. However, many applications, such as in a forest, involve large dielectric structures with losses. In this case, the assumption of perfectly conducting boundary conditions results in a lack of accuracy in predicting the actual electromagnetic field. On the other hand, the impedance

surface diffraction formulas are rather cumbersome to use for propagation prediction in a forest. Thus, the difficulty of using the rigorous solutions for propagation prediction forces simplifications to be made. Some existing diffraction coefficients modify the perfectly conducting UTD diffraction coefficient in order to make it applicable to dielectric wedges with losses. For a normal-incident plane wave, there is a general form of the perfectly conducting UTD based diffraction coefficient that includes the existing solutions as special cases of it. The general form can be expressed as

$$D(q_n)=\frac{-\exp\left[j(\frac{p}{4})\right]}{2n\sqrt{2pk}\sin\left(q-\frac{p}{m}\right)}$$
$$\left[\begin{array}{l}\cot\left(\frac{p+a_1}{2n}\right)F\left[kLa^{-}a_1\right]+\cot\left(\frac{p-a_1}{2n}\right)F\left[kLa^{-}a_1\right]\\+\cot\left(\frac{p+a_1}{2n}\right)F\left[kLa^{+}a_1\right]+\cot\left(\frac{p-a_1}{2n}\right)F\left[kLa^{+}a_1\right]\end{array}\right] \quad (17)$$

where $F(x)$ is the transition function to solve no-uniform problem for Keller, and is defined as

$$F(x)=2j\sqrt{x}\exp(jx)\int_{\sqrt{x}}^{\infty}\exp(-jt^2)dt \quad (18)$$

and the parameter of distance L is given by

$$L=s\cdot\sin^2\left(q-\frac{2p}{n}\right) \quad (19)$$

Moreover, the functions $a^{\pm}(a_1)=2\cos^2\left((2npN^{\pm}-a_1)/2\right)$ and $N^{\pm}$ is the smallest integer satisfying the following equations

$$\begin{aligned}2pnN^{+}-a_1&=p\\2pnN^{-}-a_1&=-p\end{aligned} \quad (20)$$

From (13), at least two functions among four cot function are divergent at the shadow boundary and reflection boundary. Meanwhile the corresponding transition functions go to zero, thus the singularity is removed.

Next we calculate the area of the blind region. The blind region can be calculated from GTD and the reference [11] as

$$\frac{p}{2}-a^{-\frac{1}{3}}\le q\le\frac{p}{2}+a^{-\frac{1}{3}} \quad (21)$$

where $a=(kr)^{\frac{1}{3}}$ with the wave number $k=2p/l$ and the wavelength in vacuum $l=c/f=300MHz/f$.

IV. Model Simulation Result and Analysis

We take the birch with the circumference $l=1.1m$ as example, the frequency of source point in the base station f=2.4GHz, the radius of standing tree $a=l/2p$, source and receiver are equal height, namely diameter at breast height z=1.3m. We employ equiangular polygon of eighteen to approximate the stem form. Let the distance of the secondary source point located at (x',y',z') along the negative Y axis is $y'=a$, and the location of the receiving point be located at (x',y',z') along the positive Y axis is $y_1=a\times\sin q$. The wedge angle $b=150°$, the relative dielectric constant $e_r=2.7275$ and the conductivity $s\approx 0$.

Suppose E_i is the incident field. From (12), the diffraction field E_d of the receiver satisfies $E^n(s)=E^{n-1}(Q)D(q_n)A(s)\exp(-jks)$, then considering an incident plane wave the diffraction loss of the receiver power can be written in the form

$$h=20\log\left(\frac{E_d}{E_i}\right)(dB) \quad (22)$$

The variation between the diffraction loss and the dodecagon angle (Wedge angle)is show in Fig.4. The variation between the diffraction loss and frequency of source is show in Fig.5.

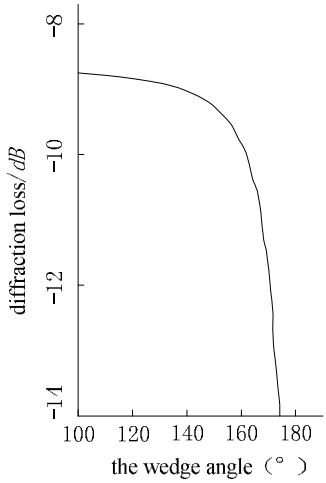

Figure 4. The variation between the diffraction loss of the receiver power and the wedge angle

Fig.4. indicates that the inverse relation between the diffraction loss of the receiver power and the wedge angle. The diffraction loss of the receiver power rapidly decreases with increasing wedge. When the wedge angle $b>150°$, the receiving antennas in the deep region of diffraction is near to the wedge plant, which agrees with the expression (11). Fig.5. shows that the diffraction loss of the receiver power decreases with the increasing frequency of source, i.e. the diffraction loss adds because the diffraction loss increases, wavelength is shortened and ability of the diffraction decreases with the increasing frequency.

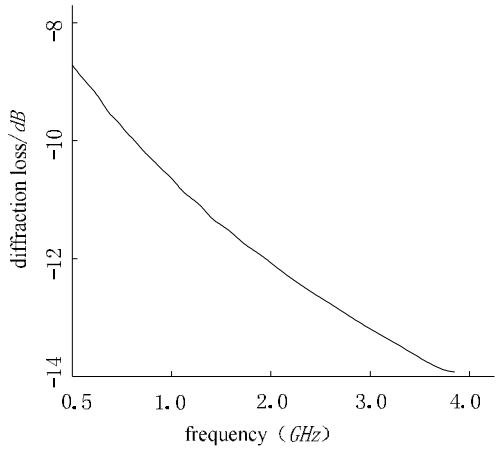

Figure 5. The variation between the diffraction loss of the receiver power and the frequency of source

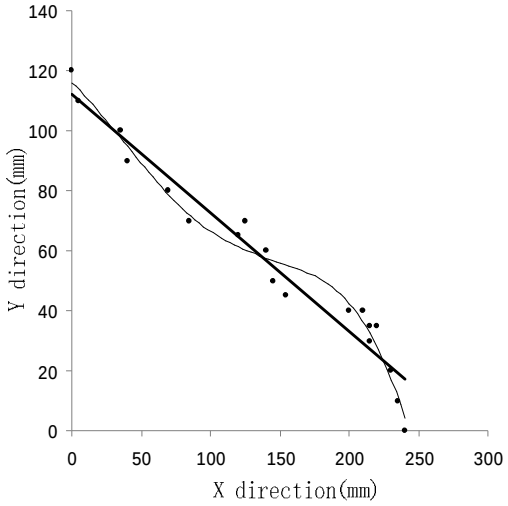

Figure 6. The experimental curve of diffraction of standing tree

The field distribution of the birch measured by the Protek3290N strength apparatus is shown in Figure.6. If the diffraction fades less than -12dB, we recognized that there is the blind region. The frequency of source is used with the amplitude 2.405GHz. The dots represent the location distribution of sample point in real. From Fig.5., by using approximation linear analysis, we have y=-0.4508x+113.49, and thus the angle of the blind region, $\alpha = arctg0.4508 = 4.27^\circ$. If we use the average error ± 3 % of basal area for breast-height, a can be written as

$$\left[k(1.03a)\right]^{-\frac{1}{3}} \le a \le \left[k(0.97a)\right]^{-\frac{1}{3}} \tag{20}$$

In our example of the birth, $l = \frac{300\times10^6}{2.405\times10^9} = \frac{1}{8.02}$, $a = 1.1/2p$. From Eq. (20), we obtain $25.6^\circ \leqslant \alpha \leqslant 26.1^\circ$.

So the theory error is $5.2\% \leqslant \eta \leqslant 7\%$ within the error region without influencing sensor networking disposal.

V. CONCLUSION

In conclusion, we discuss the layout of the sensor for the measurement of standing tree and the problem of the diffraction loss and the blind region of diffraction in optimization. The physical model of diffraction on standing tree in plantation is presented by means of the principle of Fresnel-Kirchhoff and uniform geometrical theory of diffraction (UTD) . Moreover, the expression for diffraction of standing tree is derived, the capability of diffraction loss is analyzed, and the algorithm of the blind region is discussed briefly. Finally, the feasibility and validity of UTD for computing the diffraction loss of standing tree in plantation is verified by theoretical analysis and simulation. This approach can compute, analyze and evaluate the diffraction loss field for standing tree and blind region. The algorithm for diffraction of standing tree can serve as a theoretical foundation for the optimized layout of the sensor, and introduce a novel technology for the telemetry measurement of the environmental information.

From the simulation result, the propagation loss answers to the law of the electromagnetic wave propagation. However, there is error between the theory and measurement due to the influence of vegetation and terrain etc. Therefore, this model introduced in this paper needs to further optimize. This method presented in this paper is only an initial work, more work will be done.

ACKNOWLEDGMENT

This work was supported in part by the National Natural Science Foundation of Zhejiang Province of China (Grant No. Y12C160023). And Natural Science Foundation of China (Grant No. 30972425). Corresponding author: Yun-Jie Xu.

REFERENCES

[1] Deng Hongbing, Hao Zhanqing. Study on Height Growth Model of Pinus koraiensis. Chinese Journal of Ecolony,1999,18(3),pp.19-22

[2] Barrio-Anta, Dieguez-Aranda,Ulises, Castedo-Dorado, Fernando, Alvarez-Gonzalez, JuanGabriel. Mimicking natural variability in tree height of pine species using a stochastic height-diameter relationship. New Zealand Journal of Forestry Science, 2006,36(1),pp.21-34

[3] Bardi,J.F, Villacampa,Y, Losardo,O, Borzone,H. A study of the relationship height-diameter, Advances in Ecological Sciences, Ecosystems and Sustainable Development III, 2001,(10),pp.657-666

[4] LI Wei-ming ,Lv Xiao-de ,GAO Ben-qing ,LIU Rui-xiang. Ray Path Tracing on Convex Surface with

applications to the Geometrical Theory of Diffraction.2000, 28 (9):49-51.

[5] Wonn, H.T, O'Hara, K.L. Height . diameter ratios and stability relationships for four northern Rocky Mountain tree species , Western Journal of Applied Forestry,2001,16(2),pp.87-94

[6] Sharma;Mahadev. Height-diameter equations for boreal tree species in Ontario using a mixed-effects modeling approach. Forest Ecology and Management,2007, 249(3), pp.187-198

[7] ZHANG Yu-zhu, CAO Zhi-wei, YAN Dun-liang, DAI Yu-wei.Study on Quantitative Relations Between Tree Measuring Factors of Pinus sylvestris var. mongolica Plantation on Sand Land of Nenjiang River Protection Forest Science and Technology, 2006,N0.01,pp.7-9.

[8] Xian-Yu Meng. Forest mensuration(Second Edition). China Forest Press.1995.

[9] B . B . Baker and E . T . Copson,The Mathematical Theory of Huygens Principle,2nd ed., Qxford University Press,London,1953.

[10] J . H . W hltteker . Frresnel-Kirchhoff theory applied to terrain diffraction problems, Radio Sci, 1990, 25(5),pp.837-851.

[11] Paul R. ROUSSEAU and Prabhakar PATHAK, A Time Domain Uniform Geometrical Theory of Slope diffraction for a Curved Wedge, Turk J Elec Engin, 2002,Vol.10(2),pp.385-398.

[12] Mao-Guang Wang, Geometrical Theory of Diffraction, China Xidian University Press, Beijing: 1989.

[13] Xiong-Wen , Yi-Xi Xie, Diffraction over a Flat-Topped Terrain Obstacle with Bevel Edge, Chinese Journal of Electronics,1995, Vol.23(06),pp.81-83.

[14] Youngchel Kim, B.S., M.S., On a Uniform Geometrical Theory of Diffraction based Complex Source Beam Diffraction by a Curved Wedge with Applications to Reflector Antenna Analysis, Presented in Partial Fulfillment of the Requirements for the Degree Doctor of Philosophy in the Graduate School of The Ohio State University, 2009.

[15] Pathak, Kouyoymjlanrg . A uniform geometrical theory of diffraction for an edge in a perfectly conducting surface.Proc.IEEE.1974,pp.1448-1461 .

[16] Yun-Jie Xu, Wen-Bin Li, Strength Prediction of Propagation loss in Forest Based on Genetic-SVM Classifier, 2010 Second International Conference on Future Computer and Communication, vol.03,pp. 251-254, September 2010.

[17] Henry L. Bertoni, Radio propagation for modern wireless system, Publishing House of Electronics industry. Beijing: 2002.

Yun-jie XU received B.S., M.S. and Ph.D.degrees in forest engineering from the University of Beijing Forestry of China, Beijing, China, in 1998, 2004, and 2009, respectively.

From April 2004 to Dec. 2010, he was a faculty with the School of technology , Zhejiang Agricultural & Forestry University and was promoted to be an lecturer in 2005.

His current research interests include system fault diagnosis and signal propagation in forest.

Wen-bin Li received M.S. and Ph.D. degrees in Shizuoka University and Ehime University, Japan, in 1987, and 1992, respectively, Ph.D. advisor.

From 1992 to Dec. 2011, he was a faculty with the School of technology, Beijing Forestry University and was promoted to be a professor in 2000.

His current research interests include forestry Forestry machinery automation and intelligent.